Title

Study on high-CO2 tolerant Scenedesmus sp. and its mechanism via comparative transcriptomic analysis

Authors

Huang, Bo
Shan, Ying
Yi, Tao
et al.

Publication Date

2020-12-01

DOI

10.1016/j.jcou.2020.101331

Peer reviewed

Scenedesmus showing high growth rate and lipid productivity under high CO_2 conditions

Bo Huang [a], Ying Shan [a], Tao Yi [a], Tao Tang [a, b, *], Wei Wei [a, c, *], Nigel William Trevelyan Quinn [b]

[a] CAS Key Lab of Low-Carbon Conversion Science & Engineering, Shanghai Advanced Research Institute, Chinese Academy of Sciences, 99 Haike Road, Shanghai 201210, China

[b] Earth Science Division, Lawrence Berkeley National Laboratory, 1 Cyclotron Rd, Berkeley, CA 94720, USA

[c] Center for Excellence in Urban Atmospheric Environment, Institute of Urban Environment, Chinese Academy of Sciences, Xiamen 361021, China

Abstract

The emission of carbon dioxide (CO_2) in the atmosphere at an increasingly high rate is the primary cause of global warming. The green algae *Scenedesmus* grown under 1-70 % CO_2 conditions was evaluated to determine its potential for CO_2 reduction coupled with lipid productivity. The algae showed maximum biomass (3.92 g L^{-1}) at 10 % CO_2 and high biomass (2.75 g L^{-1}) at 70% CO_2. Meanwhile, High CO_2 levels (30–70%) was favorable for accumulation of lipid and the maximum lipid productivity was about 82.9 mg L^{-1} d^{-1}. The mechanism of high CO_2 tolerance of *Scenedesmus* was discussed with transcriptome analysis. It was found that the up-regulation of antioxidative system and down-regulation of CCM resulted in the acclimation of *Scenedesmus* under high CO_2 conditions.

1. Introduction

Global warming resulting from extensive greenhouse gas (GHG) emissions due to anthropogenic activities has become of increasing concern as an environmental issue. Carbon dioxide (CO_2) emissions account for approximately three-quarters of GHG emissions (Huaman et al., 2014), and CO_2 is considered to the main gas that causes climate change (Nejat et al., 2015).

The approaches of CO_2 sequestration can be broadly categorized into physical, chemical, and biological means (Mendiara et al., 2018; Silva et al., 2015; Choi et al., 2019). Among the various strategies for mitigating CO_2, the biological sequestration of CO_2 using photosynthetic microalgae has been receiving considerable attention, as microalgae has a higher CO_2 fixation ability and produces biodiesel and bioproducts through their biomass (Adeniyi et al., 2018; Choi et al., 2019). In the microalgal-CO_2 fixation technology, performances of microalgal-CO_2 fixation and biomass production heavily depend on the culture process conditions, which includes microalgal species, physicochemical parameters and hydrodynamic parameters (Zhao et al., 2014). CO_2 concentration is one of the most critical environmental conditions in microalgal cultivation since it has important effect on the pH of the culture, and then determines the solubility and availability of CO_2 and nutrients, and has a significant influence on microalgal metabolism (Qiu et al., 2017). Previous studies mainly focused on the lower CO_2 concentrations or ambient air and the corresponding CO_2 concentrating mechanism (CCM) (Singh et al., 2014; Pronina et al., 1990). In contrast, studies on high CO_2 tolerant microalgae is scare because high CO_2 concentration has great negative effect on their biochemical activity, growth and CO_2 capture efficiency (Raeesossadati et al., 2014; Solovchenko et al., 2013; Salih et al., 2011). Watanabe et al. (1992) isolated a freshwater green alga, Chlorella sp. HA-1, which showed maximum growth at 5 and 10% CO_2 but the growth rate decreased remarkably with increasing concentration of CO_2 higher than 10%. Nakano et al. (1996) reported the *Euglena* algae had the best growth with 5% CO_2 concentration. However, the species did not grow under greater than 45% CO_2. Tang et al. (2011) reported the maximum biomass concentration of *S. obliquus* SJTU-3 and *C. pyrenoidosa* SJTU-2 under 50% CO_2 concentration were only

0.82 g L^{-1} and 0.69 g L^{-1}, respectively. It can be found that the high CO_2 concentration had great inhibition for algae growth. As such, it is necessary to select suitable algae strain with high tolerance and high growth rate under high CO_2 concentration.

The present study reported one freshwater *Scenedesmus* algae could tolerate 70% CO_2 and simultaneously showed fast growth rate and high carbon-fixing capacity. The influence of the different CO_2 concentrations on algae growth, CO_2 biofixation rate, chemical component was investigated. The tolerance mechanism of the algae for high concentration was revealed vis transcriptomic analysis.

2. Experiment

2.1 Microalgae and growth conditions

The freshwater *Scenedesmus* was separated from a water sample collected locally (Shanghai). The culture was incubated in bubble column photobioreactors (PBRs, 40 cm height, 4.5 cm diameter) with 300 ± 5 mL working volume of BG11 medium under 100 μmol $m^{-2}s^{-1}$ and 28 ± 0.5 ℃. White LEDs were used for the continuous illumination during the cultivations on one side of the PBRs and measured by a LI-250 Light Meter with a quantum sensor (SR.NO.Q49770 of QUANTUM, LI-COR, USA). The temperature was maintained using constant temperature water bath. The initial cell density in the culture was controlled around OD_{750} of 0.1 (approximately 0.07 g L^{-1}). The concentration of CO_2 was regulated by controlling the flow rates of air and CO_2 with a gas mass flow controller, respectively. The input gas was 0.2 L min^{-1} of CO_2-enriched air with different CO_2 concentration.

2.2 The effect of CO_2 concentration on microalgae growth.

In order to investigate the effect of CO_2 concentration on *Scenedesmus* growth, the algae cells were cultivated for 8 days under 1%, 10%, 20%, 30%, 50% and 70% CO_2 concentration, respectively. Samples were taken daily from the PBRs to determine the algal growth and pH of the culture medium. Generally, 12 mL of culture medium was collected in a clean glass tube, and the pH of the sample was measured by Five Easy pH meter (METTLER TOLEDO) immediately. 2 mL of the sample was used to determine the maximum quantum yield of photosystem II. The Fv/Fm was measured

using fluorescence monitoring system (FMS2, Lufthansa Scientific Instruments Co., Ltd., UK) after the sample being placed in dark conditions for 30 min (García-Cañedo et al., 2016). 10 mL of the sample was filtered using a pre-dried and pre-weighed cellulose membrane (0.45 μm pore size), washed with deionized water, dried for 24 h at 105 ℃, cooled in a desiccator and then weighed again. The dry weight of the blank filter was subtracted from that of the loaded filter to obtain the microalgae dry cell weight.

The microalgae biomass productivity and specific growth rate were calculated in order to determine the microalgae growth performance. The microalgae biomass productivity was calculated using equation (1):

$$P = \frac{X_f - X_0}{t_f - t_0} \qquad (1)$$

Where, P was the microalgae biomass productivity (g L^{-1} d^{-1}), X_f and X_0 were the cell concentrations (g L^{-1}) at the end time t_f (d) and initial time t_0 (d), respectively.

The specific growth rate (μ) was calculated with equation (2):

$$\mu = \frac{ln(X_f/X_0)}{t_f - t_0} \qquad (2)$$

where, μ was the specific growth rate (d^{-1}), X_f and X_0 were the cell concentrations (g L^{-1}) at the end time t_f (d) and initial time t_0 (d), respectively.

2.3 Measurement of CO_2 biofixation rate

The harvested microalgae were frozen, and then treated with freeze drying. The carbon content of the *Scenedesmus* cells was measured using Organic Elemental Analyzer (Thermo Flash 2000). The CO_2 biofixation rate R_{CO_2} (g L^{-1} d^{-1}) was calculated using the following equation:

$$R_{CO_2} = C_C P\left(\frac{M_{CO_2}}{M_C}\right) \qquad (3)$$

where C_C was the carbon content of the microalgal cell (%, w/w). P was the microalgae biomass productivity (g L^{-1} d^{-1}). M_C and M_{CO_2} was the molecular weight of carbon and carbon dioxide, respectively

2.4 The effect of CO_2 concentration on chemical composition of microalgae

At the end of the cultivation, 0.5 mL of sample was centrifuged at 13,400 rpm for 10 min in a 2 ml tube, the supernatant was discarded and 1 ml of deionized water was added to wash the pellet using vortex for 5-10 s. The sample was then centrifuged at 13,400 rpm for 10 min and the supernatant was discarded. The pellet was then dried with vacuum freeze-drying for 24 h. The 2 ml tube containing sample was then stored in darkness at -20 ℃ until analysis. The total carbohydrate content was analyzed by phenol-sulfuric acid method (Cheng et al., 2017). The total lipid content was measured by the colorimetric sulfo-phosphovanillin (SPV) method (Li et al., 2015). The total protein content was measured by BCA Protein Assay Kit (C503061, Sangon Biotech) with the standardized protocol.

The total lipid productivity was determined using equation (4):

$$P_{Lip} = \frac{X_f Y_{lip}}{t_f} \qquad (4)$$

Where, P_{Lip} and Y_{Lip} were the total lipid productivity and the total lipid content of the cell. X_f were the cell concentrations (g L^{-1}) at the end time t_f (d).

2.5 Transcriptomic analysis

The algal cells were collected at day 3 for *Scenedesmus* cultivated under 1% and 70% CO_2 conditions with three replicates. The sample treatment, transcriptomic determination, gene annotation and the related bioinformatics analysis were described in previous studies (Cheng et al., 2019; Li et al., 2018; Zhou et al., 2017). Two parameters were selected to investigate the target genes. If false discovery rate (FDR) was less than 0.05 and the absolute value of Log2 fold change (Log2FC) was not less than 1, the gene was regarded as significantly expressed one. The global distributions of significantly expressed genes were made on the whole genome scale using iPath 2.0 (Yamada et al., 2011) .

2.6 Statistics

All experiments were replicated three times and the results were expressed as mean ± standard deviation. A Student's t test was used to assess statistical significance. A *P* value of less than 0.05 was considered statistically significant.

3.Results

3.1 Effect of CO_2 concentration on *Scenedesmus* growth

The *Scenedesmus* strain was cultured under continuous illumination with a high flow rate (0.7 vvm) of different CO_2 concentrations ranging from 1 to 70%. The effects of different CO_2 concentrations on microalgae growth are shown in Fig. 1. Previous researches showed that the concentration of CO_2 aeration above 5% could be harmful to microalgal cells and inhibit the microalgal growth (Chiu et al., 2008; Yoo et al., 2010). In this study, the maximum biomass concentration (3.92 g L^{-1}) was obtained at 10% CO_2. Meanwhile, the algae showed short lag periods and high biomass concentrations under 20-70 % CO_2 conditions. The maximum biomass concentration, biomass productivity and specific growth under 70% CO_2 could reach up to 2.75 g L^{-1}, 0.34 g L^{-1} $d^{-1}$and 0.46 d^{-1}, respectively. Although few microalgae were able to tolerate a high-level CO_2 concentration up to 70% (Hanagate et al., 1992; Sung et al., 1999a, b; Yue et al., 2005) or even 100% (Seckbach et al., 1970), the growth parameters in this study are the highest as far as the authors known. Hanagata et al. (1992) reported that *Scenedesmus* and *Chlorella* showed high CO_2 tolerant under high CO_2 concentrations (10-80% CO_2). However, the maximum biomass concentration was only around 0.3-0.5 g L^{-1}. Ota et al. (2009) reported the maximum biomass concentration of *C. littorale* was only 0.5 g L^{-1} at 50% CO_2 after 14 d cultivation. Sung et al. (1999 a) reported one *Chlorella SP*. KR-1 strain showed maximum growth at 10% CO_2, and the maximum algae concentration was only 0.71 g L^{-1} under 70% CO_2 condition. Yue et al. (2005) reported that the maximum biomass concentration of ZY-1 strain was only 0.766 g L^{-1} after 6 days cultivation under 70 % CO_2 although much higher nitrate and phosphate concentrations (M4N culture media) were used during the cultivation. In this study, although *Scenedesmus* were cultivated under low initial cell concentration, high CO_2 concentration and high gas flow rate, the *Scenedesmus* strain showed excellent CO_2 tolerance and growth characters. These results meant that *Scenedesmus* could acclimate to the high CO_2 environment and adjusted the external environment to be suitable for growing at the same time.

3.2 Effect of CO2 concentration on carbon content and CO_2 biofixation rate of *Scenedesmus*

To evaluate the potential ability of *Scenedesmus* to sequestrate CO_2, the carbon content and CO_2 biofixation rate of *Scenedesmus* were investigated. The analysis of carbon element showed that the carbon content of the *Scenedesmus* cells were around 50 %, which did not change greatly under different CO_2 concentrations (Fig.2). The CO_2 biofixation rate R_{CO_2} (g L^{-1} d^{-1}) was calculated according to Eq. (4). As shown in Fig. 2. The highest CO_2 biofixation rate was 0.91 g L^{-1} d^{-1} under 10% CO_2 concentrations. Although CO_2 biofixation rate decreased with further increase CO_2 concentration. the biofixation rate is still as high as 0.68 and 0.64 g L^{-1} d^{-1} under 50% and 70% CO_2 concentration, respectively. The above results were similar with the *Scenedesmus* biomass concentrations. Thus, this excellent CO_2 capture ability makes the *Scenedesmus* strain a potential candidate for CO_2 sequestration.

3.3. Effect of CO_2 concentration on F_v/F_m values

Fv/Fm was measured and used as an estimate for the maximum efficiency of PSII and an indicator of stress conditions (Jaeger et al., 2014). As shown in Fig.4, the Fv/Fm values firstly increased at the initial stage and then decreased at the end stage under all the CO_2 concentrations. At initial stage, comparing to the low CO_2 concentration (1-10%), high CO_2 concentration showed lower Fv/Fm values and the Fv/Fm values decreased with CO_2 concentration increase, which meant a reduced photochemical efficiency by damage to PSII under high CO_2 stress. However, the algae could rapidly acclimate the environment and recovered normal Fv/Fm values within 3 days. The above results were consistent with the algae growth tendency.

3.4 Effect of CO_2 concentration on pH of culture medium

pH is one of the most critical environmental conditions in microalgal cultivation since it determines the solubility and availability of CO_2 and nutrients, and has a significant influence on microalgal metabolism (Chen et al., 1994). Hence, in order to determine the effect of CO_2 concentration on the pH of medium, pH during cultivation

was monitored under different CO_2 concentrations. As shown in Fig.3, a pH shift occurred in all cultures to more alkaline conditions over time. Meanwhile, the pH range of the cultivation medium decreased with increasing CO_2 concertation. Comparing to the pH range of 8.0-8.7 at 1% CO_2 concentration, the pH decreased to 6.2-7.6 with increasing CO_2 concentration to 10%, which was the optimal pH for algae growth (Moheimani et al., 2013). A significant reduction of pH value was observed for 50% and 70% CO_2 concentrations, which was in the range of 5.4-6.6 and 5.2-6.5, respectively. Generally, the pH of the culture medium was decided by the acidification resulting from CO_2 into the culture medium and the alkalization due to microalgae photosynthesis resulting in CO_2 uptake (Shiraiwa et al., 1993). Comparing to the high pH in 1% CO_2, the pH of the culture in 10% CO_2 remained in the range of 6-7, indicating that high CO_2 concentrations were able to nullify the pH increase that would be a normal consequence of high rates of photosynthesis (Varshney et al., 2016). Under high CO_2, the strengthening of acidification and the decrease of photosynthesis resulted in the low pH range comparing to 1 and 10% CO_2. However, the pH of the culture medium increased with time because the photosynthesis enhanced after algae acclimation the environment. Alkalization of the medium is believed to compensate, to a considerable extent, for the acidification effect of high CO_2 concentrations (Solovchenko et al., 2013).

3.5 Effect of CO_2 concentration on biochemical composition

Cultivation of microalgae using CO_2 not only affects its growth, but it could also affect the chemical composition distribution in its biomass (Kassim et al.2017). It is well known that protein, lipid and carbohydrate are the main three types of macromolecules in algae cells (Liu et al., 2012). In this study, the total protein, carbohydrate and lipid contents of *Scenedesmus* biomass were determined under different CO_2 concentrations. As shown in Fig. 5, the total contents of these three biochemical compounds were 86.0 % (1% CO_2), 90.6% (10% CO_2), 88.7% (20% CO_2), 86.5% (30% CO_2), 82.9% (30% CO_2) and 79.6% (30% CO_2), respectively. The highest total contents of these three biochemical compounds was found with 10% CO_2 aeration,

which corresponds to the previously mentioned findings that the highest biomass concentration and the best growth status were found with 10% CO_2.

As shown in Fig. 5, the total protein content decreased with increasing the CO_2 concentration from 1% to 30% and then slightly increased under 50% and 70% CO_2. Different from protein, the lipid content of *Scenedesmus* exhibited an increasing tendency with an increase in the CO_2 concentration and the maximum carbohydrate content was obtained at 10% CO_2 and then it decreased with furtherly increasing the CO_2 concentration. These results indicated that with a concomitant reduction in protein content, more carbohydrate accumulated under low CO_2 concentrations (10-20%) and more lipid accumulated under high CO_2 concentrations (30-70%). The results are similar with algae cultivated under nitrogen starvation to get more carbohydrate and lipid content (Zhu et al., 2014; Pancha et al., 2014; Braga et al., 2019). It is well known that the nitrogen is an essential nutrient for protein synthesis (Kolber et al., 1988). Comparing to 10-30% CO_2, the algae grew slowly under 50 and 70% CO_2 conditions and more nitrogen would exist in the culture, which resulted in the higher protein contents under 50 and 70% CO_2. The variation of carbohydrate contents is similar to Singh et al. (2016). It was reported that lowest carbohydrate proportion (18.35%) was observed with *Chlorella sp*. on 0.06% air. It was increased to 50.04% in 6% CO_2 concentration, after which it declined to 41.82% in 24% CO_2.

Microalgae have drawn great attention as promising sustainable source of lipids. As shown in Fig. 5, the lipid contents increased from 89.0 to 197.3 mg g^{-1} when CO_2 concentration increased from 1% to 30%. The lipid contents were attained around 190 mg g^{-1} furtherly increasing CO_2 concentration to 50% and 70%. The above results showed high level of CO_2 concentration improved the lipid content of microalgae, which was similar to the reports that the lipid content of Chlorella fusca and Phaeodactylum tricornutum was shown to increase when cells were grown at increasingly higher concentration of CO_2 (Dickson et al.,1969; Yongmanitchai et al., 1991). The lipid content of *Scenedesmus* is in general a moderate lipid content 10-18% (Gouveia et al., 2009; Mandal et al., 2009; Matsunaga et al., 2009; Yoo et al., 2010.; Ho et al., 2010). In this study, the total lipid content was comparable to these reports.

However, the total lipid productivities were 82.9 and 66.8 mg L^{-1} d^{-1} under 30 and 70 % CO_2, respectively, which was about 2.4 and 1.9 times comparing to that 35.1 mg L^{-1} d^{-1} reported by Ho et al. (2010). Of course, in order to enhance the economic feasibility of microalgal biodiesel, it is necessary to develop the ‘‘fattening” strategy (Pancha et al., 2015; Yu et al., 2018; Liao et al., 2018) to enhance lipid accumulation to achieve a higher lipid content/productivity, an appropriate composition of fatty acid profiles as well as higher CO_2 consumption rate.

3.6 The mechanism of high CO_2 tolerance of Scenedesmus

3.6.1 Global transcriptional changes of *Scenedesmus* in response to high CO_2

The mechanism of high CO_2 tolerance of *Scenedesmus* was investigated by comparative transcriptomic analysis. *Scenedesmus* was cultivated under 70% and 1% CO_2, respectively, and collected at day 3 for further transcriptomic analysis. Totally, there were 10, 4116 unigenes were detected for the two groups cells. To identify genes that displayed significant changes in expression under high CO_2 stress, differentially expressed genes (DEGs) were analyzed by comparing the libraries of 70% and 1% CO_2 cultivation algae. In all, the abundance of 13, 364 filtered unigenes (FDR <0.05 and $|\log2FC| \geq 1$) of varying overall length showed evidence of differential transcription. As shown in Fig. 6, a high number of genes were down-regulated than up-regulated in response to high CO_2 stress. A total of 9002 down-regulated and 4362 up-regulated DEGs were detected after exposure 70% CO_2 for 3days.The global distributions of these genes are shown in Fig. 7. Red lines represented the up-regulated genes and blue lines represented the down-regulated genes. Overall, some genes in Photosynthesis - antenna proteins, Photosynthesis, Ribosome, Starch and sucrose metabolism, Carbon fixation in photosynthetic organisms, Oxidative phosphorylation and Porphyrin and chlorophyll metabolism were significantly down-regulated. At the same time, some genes in Ribosome biogenesis in eukaryotes, Glyoxylate and dicarboxylate metabolism, Citrate cycle (TCA cycle), DNA replication, Proteasome, Carbon fixation in

photosynthetic organisms and many amino acids metabolism were significantly up-regulated.

3.6.2 Genes involved in antioxidant system regulated high CO_2 stress conditions

The low pH due to high CO_2 may induce high oxidative stress and lead to production of reactive oxygen species (ROS) in microalgae cells, which is possible to make serious damages to microalgae (Mallick et al., 2000; Yangüez et al., 2015; Brutemark et al., 2015). Establishment of an anti-oxidative system represents one of the most important strategies for algae adaptation to oxidative stress (Puckette et al., 2007; Zhou et al., 2009). Within cells, superoxide dismutase (SOD) acts as the first line to defense that catalyzes the dismutation of superoxide (O_2^-) into oxygen (O_2) and hydrogen peroxide (H_2O_2) (McCord et al., 1988). Catalase (CAT), Glutathione peroxidase (GPX) and Ascorbate peroxidase (APX) are considered the most important enzymes to catalyze the transformation of H_2O_2 to H_2O (Nakano et al., 1981; Livingstone et al., 2001) . As shown in Figure 9, CAT can energy-efficiently degrade H_2O_2 without consuming cellular reducing equivalents. In contrast to CAT, APX and GPX can detoxify H_2O_2 to H_2O in the glutathione-ascorbate cycle and glutathione-peroxidase cycle using glutathione (GSH) as the reductant, respectively. In this study, the transcription of SOD2, APX and CAT were up-regulated (Table 1) under 70% CO_2 conditions. However, the expression of GPX was down-regulated, which means that SOD, APX and GAT is the preferred way to relieve the harmful radicals.

In addition to antioxidant enzymes, some non-enzymatic components can also be produced to alleviate ROS (Mallick et al., 2000). Glutathione (GSH) is a pivotal compound to direct scavenging of ROS (Jaeger et al., 2018) . GSH is synthesized via γ-glutamylcysteine synthetase (γ-GCSTT) and glutathione synthetase (GSHSTT) through two steps. As shown in Table 1, the up-regulation of γ-GCSTT and no change of GSHSTT indicated that more GSH produced under high CO_2 conditions. In addition to direct scavenging of ROS, GSH can also function as the reductant in the glutathione-ascorbate cycle and glutathione-peroxidase cycle, which can be oxidized to glutathione disulfide (GSSG). The ratio between GSH and GSSG depends on the activity of the

GSH reductase (GR) enzyme (Apel et al., 2004). As shown in Table 1, the log2FC of GR is 1.26, which means GSH reductase enzyme will have high activity and high ratio of GSH will exist in the cells (Martindale et al., 2002). These findings indicate that high CO_2 induces oxidative stress potentially through the activation of antioxidative enzymes including SOD, CAT and APX and biosynthesis of GSH to reduce the ROS.

3.6.3 Differentially expressed genes related to photosynthesis and carbon fixation

High CO_2 induces high stress and it is possible to make serious damages to microalgae photosynthesis. Just as shown in Fig. 8, the down-regulations of *PsaD*, *PsaE*, *PsaF*, *PsaG*, *PsaH*, *PsaI*, *PsaK*, *PsaL*, *PsaN* and *PsaO* (photosystem I), *PetE* and *PetH* (photosynthetic electron transport), *PsbO*, *PsbP*, *PsbQ*, *Psb R*, *PsbW*, *PsbY*, *Psb27* and *Psb28* (photosystem II) indicated that the photosynthesis activity was declined. It was consistent with the maximum quantum yield of photosystem II from day 0 to day 3 (Fig. 4) and the down regulations of LHCA1-5 and LHCB2, 4, 5 of antenna proteins (Table 2) which is important in photosynthesis for light harvesting (Kim et al., 2010). It meant that *Scenedesmus* cells acclimated to high CO_2 stress by temporarily sacrificing photosynthetic efficiency to maintain their stability.

There were three kinds of possible CO_2 fixation pathways, Calvin- Benson cycle (C3 photosynthetic pathway), C4-dicarboxylic acid cycle (C4 photosynthetic pathway) and crassulacean acid metabolism (CAM) pathway (Fan et al., 2016; Li et al., 2017). As shown in Table 3, most of the enzymes involved in these pathways were downregulated under 70% CO_2. The results indicated that the whole carbon fixation process was inhibited by high CO_2 stress, which was consistent with the relative lower growth rate and photosynthesis activity of *Scenedesmus* compring to that of 1% CO_2. However, the relative expressions of ribulose-bisphosphate carboxylase large chain (rbcL) was up-regulated involved in C3 pathways. Ribulose-1,5-bisphosphate carboxylase−oxygenase (Rubisco), the first and critical enzyme of the Calvin cycle (Spreitzer et al., 2002). Rubisco is only activated when CO_2 concentration is greater than its *K*m (CO_2) because CO_2 is the only carbon source that rubisco can utilize (Cheng

et al., 2013). In this study, under high CO_2, the pH in the first 3 days was around 5.20-5.72 and the vast majority of carbon in the culture is in the form of CO_2 (aq) (Zhao et al., 2014).CO_2 (aq) can directly permeate intracellular pyrenoids and resulted in upregulating the relative expressions of rbcL.

Under limit CO_2 conditions, algae generally use CCM to increase the concentration of CO_2 for Rubisco (Kupriyanova et al., 2015). The CCM can be divided into two phases as shown the CCM model by Pronina et al. (1981, 1990). As shown in Fig. 10, the first phase involves acquiring CO_2 and HCO_3^- from the culture medium and then delivering them to chloroplast, which includes CAH1 and possibly CAH8 in the periplasmic space and CAH9 in the cytoplasm. In this study, the expression of CAH1 and CAH8 was down-regulation and up-regulation, respectively. Partial CO_2 converted to HCO_3^-, which was because CO_2 (aq) is the dominant form of carbon sources. The second phase includes CAH6 located in the chloroplast stroma and CAH3 located within the thylakoid lumen. In the meantime, the CAH3 and CAH6 were down-regulated because only small amounts of HCO_3^- was delivered into the chloroplast stroma and thylakoid lumen. Especially, CAH3 in thylakoid plays an essential role in the CCM and can converse the HCO_3^- to CO_2 which is directly used by rubisco. These results were consistent with previous reports that elevating CO_2 concentration decreased CAs activity (Moroney et al., 2007). In this study, under high CO_2 condition, rubisco could get enough CO_2 supply and CCM was inhibited, which was important for the algae high CO_2 tolerant. Firstly, CCMs are energetically expensive, so at a sufficient CO_2 concentration, a down-regulation of their activity can occur, leading to energy saving (Yang et al., 2012), which may result in an enhancement of algae growth (Iñiguez et al., 2015). In addition, inhibition or down-regulation of CCM will hinder the use of bicarbonate and reduce the resulting decrease in intracellular pH (Solovchenko et al., 2013). These two reasons are important for *Scenedesmus* acclimating the high CO_2 conditions.

4 Conclusion

In this work, *Scenedesmus* were cultivated with different CO_2 concentrations from 1% to 70 % to examine the CO_2 tolerance, CO_2 biofixation abilities and lipids production. The maximum CO_2 biofixation rate and biomass concentration were obtained at 10% CO2. The algae could tolerant 70% CO2 and had great biomass concentration and lipid productivity under high CO_2 conditions. The high CO_2 tolerance mechanism of *Scenedesmus* were discussed with transcriptome analysis. The up-regulation of antioxidative enzymes and biosynthesis of GSH to reduce the ROS. The down-regulation of CCM saved the energy for photosynthesis and maintained the intracell pH. The results suggested that *Scenedesmus* has great potential for CO_2 biofixation and biodiesel production.

References

Adeniyi, O.M., Azimov, U., Burluka, A., 2018. Algae biofuel: Current status and future applications. Renew. Sust. Energ. Rev. 90, 316-335.

Apel, K., Hirt, H., 2004. Reactive oxygen species: metabolism, oxidative stress, and signal transduction. Annu. Rev. Plant. Biol. 55, 373-399.

Braga, V.D.S., Moreira, J.B., Costa, J.A.V., Morais, M.G.D., 2019. Enhancement of the carbohydrate content in Spirulina by applying CO_2, thermoelectric fly ashes and reduced nitrogen supply. Int. J. Biol. Macromol. 123, 1241-1247.

Brutemark, A., Engström-Öst, J., Vehmaa, A., Gorokhova, E., 2015. Growth, toxicity and oxidative stress of a cultured cyanobacterium (*Dolichospermum* sp.) under different CO_2/pH and temperature conditions. Phycol. Res. 63, 56-63.

Chen, C.Y., Durbin, E.G., 1994. Effects of pH on the growth and carbon uptake of marine phytoplankton. Mar. Ecol. Prog. Ser. 109, 83-94.

Cheng, D.J., Li, X.Y., Yuan, Y.Y., Yang, C.Y., Tang, T., Zhao, Q.Y., Sun, Y.H., 2019. Adaptive evolution and carbon dioxide fixation of *Chlorella* sp. in simulated flue gas. Sci. Total. Environ. 650, 2931-2938.

Cheng, D.J., Li, D.J., Yuan, Y.Y., Zhou, L., Li, X.Y., Wu, T., Wang, L., Zhao, Q.Y., Wei, W., Sun, Y.H., 2017. Improving carbohydrate and starch accumulation in

Chlorella sp. AE10 by a novel two-stage process with cell dilution. Biotechnol. Biofuels. 10, 75.

Cheng, J., Huang, Y., Feng, J., Sun, J., Zhou, J., Cen, K., 2013. Mutate *Chlorella* sp. by nuclear irradiation to fix high concentrations of CO_2. Bioresour. Technol. 136, 496-501.

Chiu, S.Y., Kao, C.Y., Chen, C.H., Kuan, T.C., Ong, S.C., Lin, C.S., 2008. Reduction of CO_2 by a high-density culture of *Chlorella* sp. in a semicontinuous photobioreactor. Bioresour. Technol. 99(9), 3389-3396.

Choi, Y.Y., Patel, A.K., Hong, M.E., Chang, W.S., Sim, S.J., 2019. Microalgae Bioenergy with Carbon Capture and Storage (BECCS): An emerging sustainable bioprocess for reduced CO_2 emission and biofuel production. Bioresour. Technol. Reports. 7, 100270.

Dickson, L.G., Galloway, R.A., Patterson, G.W., 1969. Environmentally-Induced Changes in the Fatty Acids of Chlorella. Plant. Physiol. 44(10), 1413-1416.

Fan, J.H., Xu, H., Li, Y.G., 2016. Transcriptome-based global analysis of gene expression in response to carbon dioxide deprivation in the green algae *Chlorella pyrenoidosa*. Algal. Res. 16, 12-19.

García-Cañedo, J.C., Cristiani-Urbina, E., Flores-Ortiz, C.M., Ponce-Noyola, T., Esparza-García, F., Cañizares-Villanueva, R.O., 2016. Batch and fed-batch culture of *Scenedesmus incrassatulus*: Effect over biomass, carotenoid profile and concentration, photosynthetic efficiency and non-photochemical quenching. Algal. Res. 13, 41-52.

Gouveia, L., Oliveira, A.C., 2009. Microalgae as a raw material for biofuels production. J. Ind. Microbiol. Biotechnol. 36(2), 269-274.

Hanagata, N., Takeuchi, T., Fukuju, Y., Barnes, D.J., Karube, I., 1992. Tolerance of microalgae to high CO_2 and high temperature. Phytochemistry. 31(10), 3345-3348.

Ho, S.H., Chen, W.M., Chang, J.S., 2010. *Scenedesmus obliquus* CNW-N as a potential candidate for CO_2 mitigation and biodiesel production. Bioresour. Technol. 101(22), 8725-8730.

Huaman, R.N.E., Jun, T.X., 2014. Energy related CO_2 emissions and the progress on CCS projects: a review. Renew. Sust. Energ. Rev. 31, 368-385.

Iñiguez, C., Carmona, R., Lorenzo, M.R., Niell, F.X., Wiencke, C., Gordillo, F.J.L., 2016. Increased CO_2 modifies the carbon balance and the photosynthetic yield of two common Arctic brown seaweeds: *Desmarestia aculeata* and *Alaria esculenta*. Polar. Biology. 39(11), 1979-1991.

Jaeger, L.D., Carreres, B.M., Springer, J., Schaap, P.J., Eggink, G., Martins, D.S.V.A.P., Wijffels, R.H., Martens, D.E., 2018, *Neochloris oleoabundans* is worth its salt: Transcriptomic analysis under salt and nitrogen stress. Plos. One. 13(4), e0194834.

Jaeger, L.D., Verbeek, R.E., Draaisma, R.B., Martens, D.E., Springer, J., Eggink, G., Wijffels, R.H., 2014. Superior triacylglycerol (TAG) accumulation in starchless mutants of *Scenedesmus obliquus*: (I) mutant generation and characterization. Biotechnol. Biofuels. 7, 69.

Kassim, M.A., Meng, T.K., 2017. Carbon dioxide (CO_2) biofixation by microalgae and its potential for biorefinery and biofuel production. Sci. Total. Environ. 584-585, 1121-1129.

Kim, M.J., Park, S., Polle, J.E.W., Jin, E.S., 2010. Gene expression profiling of *Dunaliella* sp. acclimated to different salinities. Phycol. Res. 58(1), 17-28.

Kolber, Z., Zehr, J., Falkowski, P., 1988. Effects of growth irradiance and nitrogen limitation on photosynthetic energy conversion in photosystem II. Plant. Physiol. 88 (3), 923-929.

Kupriyanova, E.V., Samylina, O.S., 2015. CO_2-concentrating mechanism and its traits in *Haloalkaliphilic cyanobacteria*. Microbiology. 84(2), 112-124.

Li, D.J., Wang, L., Zhao, Q.Y., Wei, W., Sun, Y.H., 2015. Improving high carbon dioxide tolerance and carbon dioxide fixation capability of *Chlorella* sp. by adaptive laboratory evolution. Bioresour. Technol. 185, 269-275.

Li, K., Cheng, J., Lu, H.X., Yang, W.J., Zhou, J.H., Cen, K.F., 2017. Transcriptome-based analysis on carbon metabolism of *Haematococcus pluvialis* mutant under 15% CO_2. Bioresour. Technol. 233, 313-321.

Li, X.Y., Yuan, Y.Y., Cheng, D.J., Gao, J., Kong, L.Z., Zhao, Q.Y., 2018. Exploring stress tolerance mechanism of evolved freshwater strain, *Chlorella* sp. s30 under 30g/L salt. Bioresour. Technol. 250, 495-504.

Liao, Q., Chang, H.X., Fu, Q., Huang, Y., Xia, A., Zhu, X., Zhong, N.B., 2018. Physiological-phased kinetic characteristics of microalgae *Chlorella vulgaris* growth and lipid synthesis considering synergistic effects of light, carbon and nutrients. Bioresour. Technol. 250, 583-590.

Liu, W.H., Huang, Z.W., Li, P., Xia, J.F., Chen, B., 2012. Formation of triacylglycerol in *Nitzschia closterium* f. minutissima under nitrogen limitation and possible physiological and biochemical mechanisms. J. Exp. Mar. Biol. Ecol. 418-419, 24-29.

Livingstone, D.R., 2001. Contaminant-stimulated reactive oxygen species production and oxidative damage in aquatic organisms. Mar. Pollut. Bull. 42(8), 656-666.

Mallick, N., Mohn, F.H., 2000. Reactive oxygen species: response of algal cells. J. Plant. Physiol. 157(2), 183-193.

Mandal, S., Mallick, N., 2009. Microalga *Scenedesmus obliquus* as a potential source for biodiesel production. Appl. Microbiol. Biotechnol. 84(2), 281-291.

Martindale, J.L., Holbrook, N.J., 2002. Cellular response to oxidative stress: signaling for suicide and survival. J. Cell. Physiol. 192(1), 1-15.

Matsunaga, T., Matsumoto, M., Maeda, Y., Sugiyama, H., Sato, R., Tanaka, T., 2009. Characterization of marine microalga, *Scenedesmus* sp strain JPCC GA0024 toward biofuel production. Biotechnol. Lett. 31(9), 1367-1372.

McCord, J.M., Fridovich, I., 1988. Superoxide dismutase: the first twenty years (1968–1988). Free. Radic. Bio. Med. 5(5-6), 363-369.

Mendiara, T., García-Labiano, F., Abad, A., Gayán, P., de Diego, L.F., Izquierdo, M.T., Adánez, J., 2018. Negative CO_2 emissions through the use of biofuels in chemical looping technology: A review. Appl. Energ. 232, 657-684.

Moheimani, N.R., 2013. Inorganic carbon and pH effect on growth and lipid productivity of *Tetraselmis suecica* and *Chlorella* sp. (Chlorophyta) grown outdoors in bag photobioreactors. J. Appl. Phycol. 25(2), 387-398.

Moroney, J.V., Ynalvez, R.A., 2007. Proposed Carbon Dioxide Concentrating Mechanism in *Chlamydomonas reinhardtii*. Eukaryot. Cell. 6(8), 1251-1259.

Mukherjee, M., Misra, S., 2018. A review of experimental research on Enhanced Coal Bed Methane (ECBM) recovery via CO_2 sequestration. Earth-Sci. Rev.179, 392-410.

Nakano, Y., Asada, K., 1981. Hydrogen peroxide is scavenged by ascorbatespecific peroxidase in spinach chloroplasts. Plant. Cell. Physiol. 22(5), 867-880.

Nakano, Y., Miyatake, K., Okuno, H., Hamazaki, K., Takenaka, S., Honami, N., Kiyota, M., Aiga, I., Kondo, J., 1996. Growth of photosynthetic algae Euglena in high CO_2 conditions and its photosynthetic characteristics. Acta. Hortic. 440, 49-54.

Nejat, P., Jomehzadeh, F., Taheri, M.M., Gohari, M., Majid, M.Z.A., 2015. Global review of energy consumption, CO_2 emissions and policy in the residential sector (with an overview of the top ten CO_2 emitting countries). Renew. Sust. Energ. Rev. 43, 843-862.

Ota, M., Kato, Y., Watanabe, H., Watanabe, M., Sato, Y., Smith, R.L., Inomata, H., 2009. Fatty acid production from a highly CO_2 tolerant alga, *Chlorocuccum littorale*, in the presence of inorganic carbon and nitrate. Bioresour. Technol. 100(21), 5237-5242.

Pancha, I., Chokshi, K., George, B., Ghosh, T., Paliwal, C., Maurya, R., Mishra, S., 2014. Nitrogen stress triggered biochemical and morphological changes in the microalgae *Scenedesmus* sp. CCNM 1077. Bioresour. Technol. 156, 146-154.

Pancha, I., Chokshi, K., Maurya, R., Trivedi, K., Patidar, S.K., Ghosh, A., Mishra, S., 2015. Salinity induced oxidative stress enhanced biofuel production potential of microalgae *Scenedesmus* sp. CCNM 1077. Bioresour. Technol. 189, 341-348.

Pronina, N.A., Ramazanov, Z.M., Semenenko, V.E., 1981. Carbonic anhydrase activity of Chlorella cells as a function of CO_2 concentration. Sov. Plant. Physiol. 28(3), 345-351.

Pronina, N.A., Semenenko, V.E., 1990. Membrane-bound carbonic anhydrase takes part in CO_2 concentration in algal cells. Curr. Res. Photosynth. 4(18), 489-492.

Pruvost, J., Vooren, G.V., Gouic, B.L., Couzinet-Mossion, A., Legrand, J., 2011. Systematic investigation of biomass and lipid productivity by microalgae in photobioreactors for biodiesel application. Bioresour. Technol. 102(1), 150-158.

Puckette, M.C., Weng, H., Mahalingam, R., 2007. Physiological and biochemical responses to acute ozone-induced oxidative stress in *Medicago truncatula*. Plant. Physiol. Bioch. 45(1), 70-79.

Qiu, R.H., Gao, S., Lopez, P.A., Ogden, K.L., 2017. Effects of pH on cell growth, lipid production and CO_2 addition of microalgae *Chlorella sorokiniana*. Algal. Res. 28, 192-199.

Raeesossadati, M.J., Ahmadzadeh, H., McHenry, M.P., Moheimani, N.R., 2014. CO_2 bioremediation by microalgae in photobioreactors: Impacts of biomass and CO_2 concentrations, light, and temperature. Algal. Res. 6, 78-85.

Salih, F.M., 2011. Microalgae tolerance to high concentrations of carbon dioxide: A review. J. Environ. Prot. 2, 648-654.

Seckbach, J., Baker, F.A., Shugarman, P.M., 1970. Algae thrive under pure CO_2. Nature. 227, 744-745

Shailendra, S.K., Rahman, M.A., Dixit, K., Nath, A., Sundaram, S., 2016. Evaluation of promising algal strains for sustainable exploitation coupled with CO_2 fixation. Environ. Technol. 37(5), 613-622.

Shiraiwa, Y., Goyal, A., Tolbert, N.E., 1993. Alkalization of the medium by unicellular green algae during dissolved inorganic carbon. Plant. Cell. Physiol. 34(5), 649-657.

Silva, G.P.D., Ranjith, P.G., Perera, M.S.A., 2015. Geochemical aspects of CO_2 sequestration in deep saline aquifers: A review. Fuel. 155(1), 128-143.

Singh, S.P., Singh, P., 2014. Effect of CO_2 concentration on algal growth: A review. Renew. Sust. Energ. Rev. 38, 172-179.

Solovchenko, A., Khozin-Goldberg, I., 2013. High-CO_2 tolerance in microalgae: possible mechanisms and implications for biotechnology and bioremediation. Biotechnol. Lett. 35(11), 1745-1752.

Spreitzer, R.J., Salvucci, M.E., 2002. Rubisco: structure, regulatory interactions, and possibilities for a better enzyme. Annu. Rev. Plant. Biol. 53, 449-475.

Sung, K.D., Lee, J.S., Shin, C.S., Park, S.C., 1999 a. Isolation of a new highly CO_2 tolerant fresh water Microalgae *Chlorella* sp. KR-1. Renew. Energ. 16(1-4), 1019-1022.

Sung, K.D., Lee, J.S., Shin, C.S., Park, S.C., Chio, M.J., 1999 b. CO_2 fixation by *Chlorella* sp. KR-1 and its cultural characteristics. Bioresour. Technol. 68(3), 269-273.

Tang, D.H., Han, W., Li, P.L., Miao, X.L., Zhong, J.J., 2011. CO_2 biofixation and fatty acid composition of *Scenedesmus obliquus* and *Chlorella pyrenoidosa* in response to different CO_2 levels. Bioresour. Technol. 102(3), 3071-3076.

Varshney, P., Sohoni, S., Wangikar, P.P., Beardall, J., 2016. Effect of high CO_2 concentrations on the growth and macromolecular composition of a heat-and high-light-tolerant microalga. J. Appl. Phycol. 28(5), 2631-2640.

Watanabe, Y., Ohmura, N., Saiki, H., 1992. Isolation and determination of cultural characteristics of microalgae which functions under CO_2 enriched atmosphere. Energ. Convers. Manage. 33(5-8), 545-552.

Yamada, T., Letunic, I., Okuda, S., Kanehisa, M., Bork, P., 2011. IPath2.0: interactive pathway explorer. Nucleic. Acids. Res. 39, W412-W415.

Yangüez, K., Lovazzano, C., Contreras-Porcia, L., Ehrenfeld, N., 2015. Response to oxidative stress induced by high light and carbon deoxidate (CO_2) in the biodiesel producer model *Nannochloropsis salina* (Ochrophyta, Eustigmatales). Rev. biol. mar. oceanogr. 50(S1), 163-175.

Yoo, C., Jun, S.Y., Lee, J.Y., Ahn, C.Y., Oh, H.M., 2010. Selection of microalgae for lipid production under high levels carbon dioxide. Bioresour. Technol. 101(1), S71–S74.

Yu, Z., Pei, H.Y., Jiang, L.Q., Hou, Q.J., Nie, C.L., Zhang, L.J., 2018. Phytohormone addition coupled with nitrogen depletion almost tripled the lipid productivities in two algae. Bioresour. Technol. 247, 904-914.

Yue, L.H., Chen, W.G., 2005. Isolation and determination of cultural characteristics of a new highly CO_2 tolerant fresh water microalgae. Energ. Convers. Manage. 46(11-12), 1868-1876.

Zhao, B.T., Su, Y.X., 2014. Process effect of microalgal-carbon dioxide fixation and biomass production: A review. Renew. Sust. Energ. Rev.31, 121-132.

Zhou, L., Cheng, D.J., Wang, L., Gao, J., Zhao, Q.Y., Wei, W., Sun, Y.H., 2017. Comparative transcriptomic analysis reveals phenol tolerance mechanism of evolved *Chlorella* strain. Bioresour. Technol. 227, 266-272.

Zhou, Z.S., Guo, K., Elbaz, A.A., Yang, Z.M., 2009. Salicylic acid alleviates mercury toxicity by preventing oxidative stress in roots of *Medicago sativa*. Environ. Exp. Bot. 65(1), 27-34.

Zhu, S.N., Wang, Y.J., Huang, W., Xu, J., Wang, Z.M., Xu, J.L., Yuan, Z.H., 2014. Enhanced accumulation of carbohydrate and starch in *Chlorella zofingiensis* induced by nitrogen starvation. Appl. Biochem. Biotechnol. 174(7), 2435-2445.

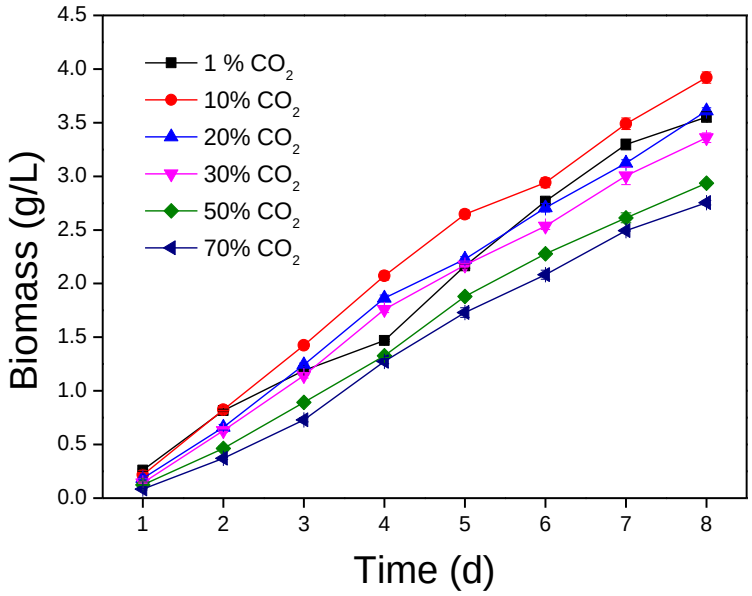

Figure 1. Time course of biomass concentration for *Scenedesmus* cultivated under 1-70 % CO_2 concentration

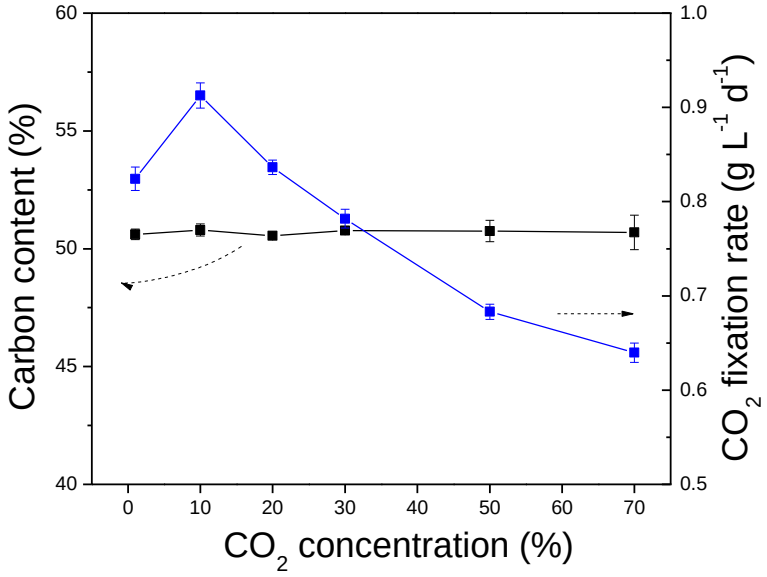

Figure 2. The carbon content (%) and CO_2 biofixation rate (R_{CO_2}, g L^{-1} d^{-1}) of *Scenedesmus* strain under different CO_2 concentrations.

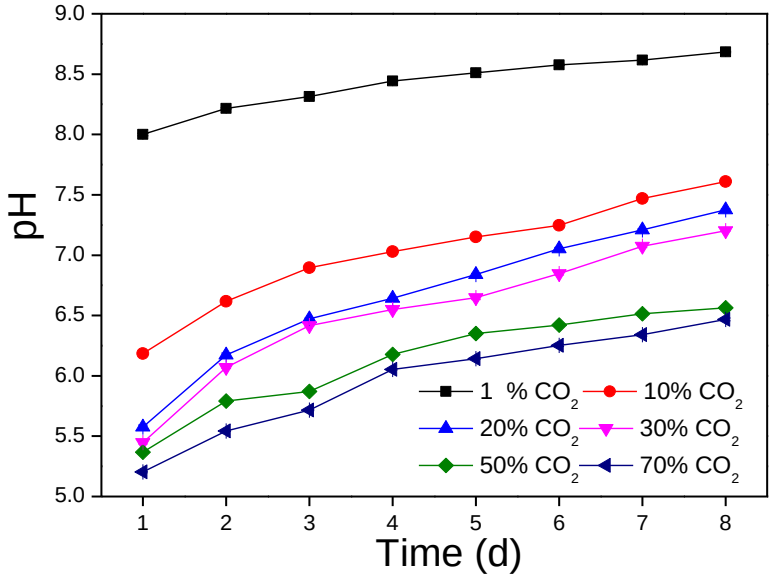

Figure 3. pH value profiles from cultivations using different CO_2 concentrations

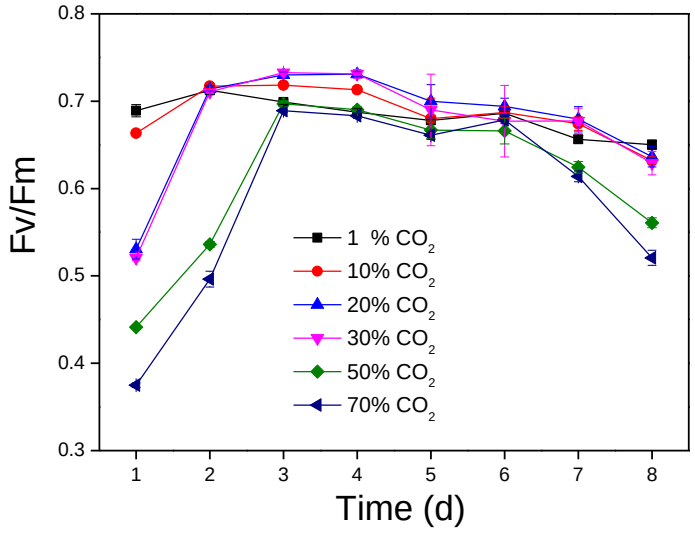

Figure 4. Fv/Fm value profiles from cultivations using different CO_2 concentrations

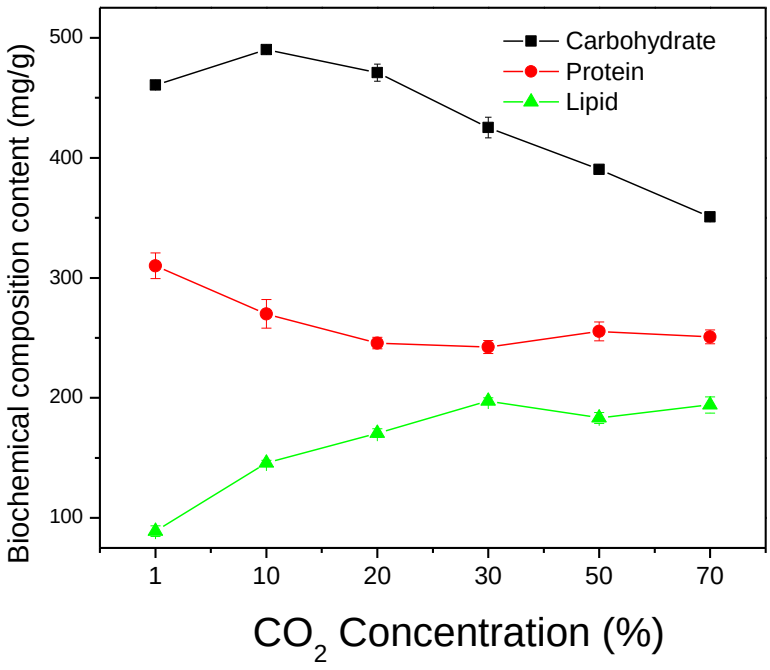

Figure 5. Time course of biochemical composition content for *Scenedesmus* cultivated under 1-70 % CO_2 concentration

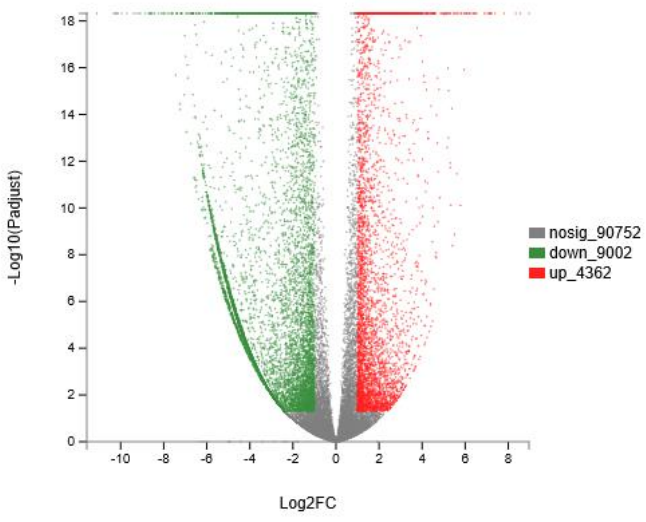

Figure 6. DEGs in the algae cells under high CO_2 stress. The number of DEGs identified in each library contrast by applying a threshold of the ratio change≥2 and q-adjust<0.05. scatter plot of DEGs (FDR <0.05and $|\log_2 FC| \geq 1$) illustrating the full set of genes samples. Red points are up-regulated genes, black points are non-DEGs, and green points are down-regulated genes.

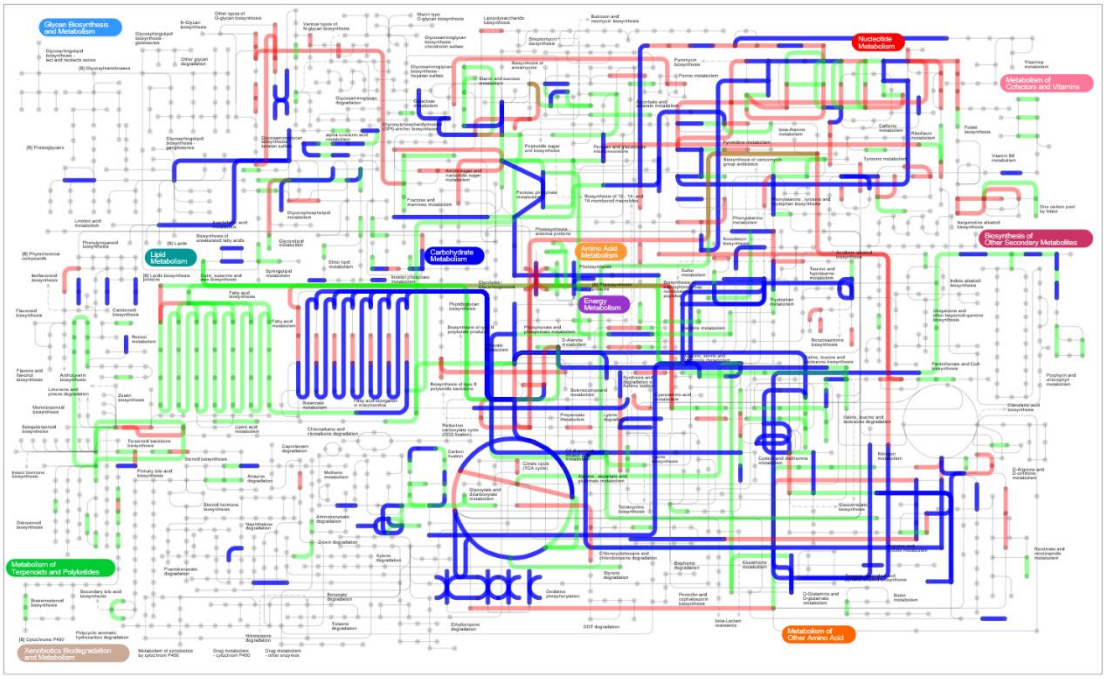

Figure 7. Global distribution of the significantly up-regulated (red) and down-regulated (green) genes in whole metabolic network of *Scenedesmus* under 1% and 70% CO_2. The red line means significantly up-regulated genes and the green line means significantly down-regulated genes. The blue lines mean they were not significantly changed. (For interpretation of the references to color in this figure legend, the reader is referred to the web version of this article.)

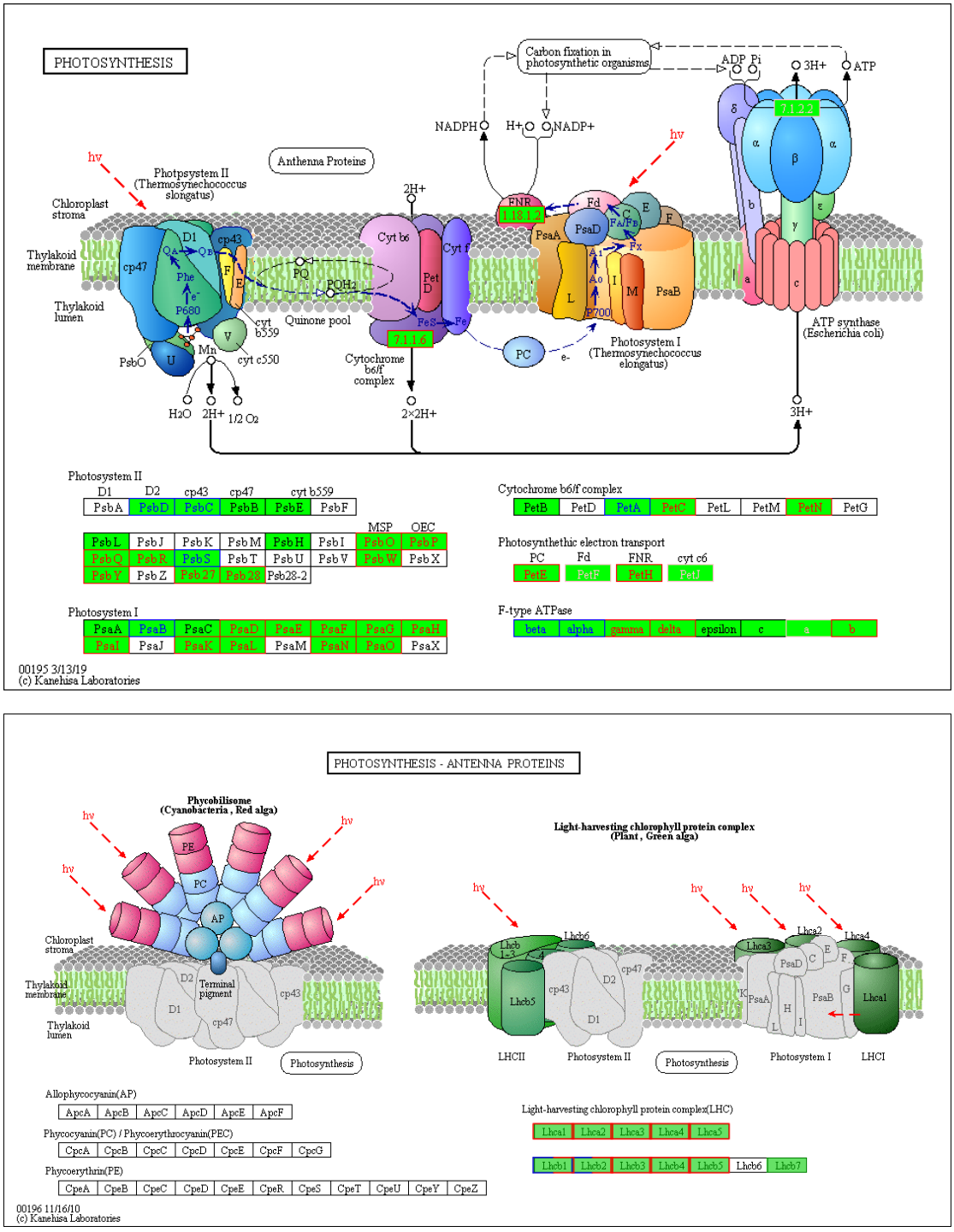

Figure 8. Comparative transcriptomic analysis for the related genes of photosynthesis (A) and photosynthesis (B) antenna protein of *Scenedesmus* under 1% and 70% CO_2. The blue frame means up-regulated genes and the red frame means down-regulated genes. The pathway maps were adapted from KEGG pathway database. (For interpretation of the references to color in this figure legend, the reader is referred to the web version of this article.)

Superoxide Dismutase:

$$2O_2^{\cdot -} + 2H^+ \xrightarrow{SOD} H_2O_2 + O_2$$

Catalase:

$$H_2O_2 \xrightarrow{CAT} H_2O + {}^1/_2\, O_2$$

Ascorbate-Glutathione Cycle:

$$H_2O_2 + \text{Ascorbate} \xrightarrow{\text{APX}} H_2O + \text{Monodehydroascrobate (MDA)}$$

$$\text{MDA} + \text{NAD(P)H} \xrightarrow{\text{MDAR}} \text{Ascorbate} + \text{NAD(P)}^+$$

$$Dehydroascorbate + GSH \xrightarrow{DHAR} Ascorbate + GSSG$$

$$\text{GSSG} + \text{NAD(P)H} \xrightarrow{\text{GR}} \text{GSH} + \text{NAD(P)}^+$$

Glutathione-Peroxidase Cycle:

$$H_2O_2 + \text{GSH} \xrightarrow{\text{GPX}} H_2O + \text{GSSG}$$

$$\text{GSSG} + \text{NAD(P)H} \xrightarrow{\text{GR}} \text{GSH} + \text{NAD(P)}^+$$

Figure 9. The principal modes of enzymatic ROS scavenging by superoxide dismutase, catalase, ascorbate-glutathione cycle and glutathione-peroxidase cycle.

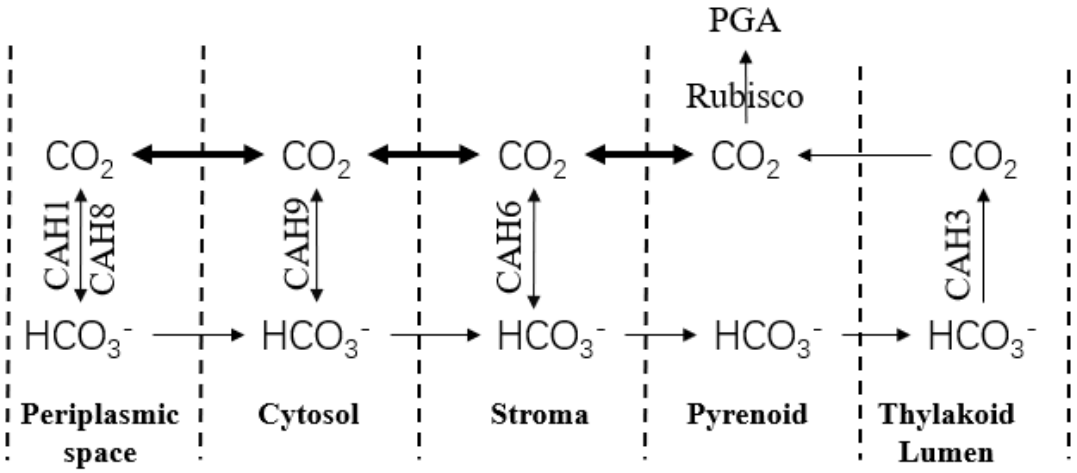

Figure 10. Models of CO_2 transport pathway of *Scenedesmus*. The thick line represents the CO_2 transport pathway under high concentrations of CO_2.

Table 1. Comparative transcriptomic analysis for the related genes of antioxidant system of *Scenedesmus* under 70% and 1% CO_2 conditions.

Gene name	Enzeyme	Log_2FC(70%/1%)	FDR
SOD2	superoxide dismutase	1.98	2.3E-98
		-4.81	1.3E-12
APX	ascorbate peroxidase	1.09	5.7E-26
		2.16	5.1E-03
		-3.65	7.5E-04
CAT	catalase	1.31	3.5E-50
GPX	glutathione peroxidase	-5.99	3.0E-11
GR	glutathione reductase	1.26	1.7E-18
γ-GCSTT	gamma-glutamylcysteine synthetase	1.49	8.9E-37
GSHSTT	glutathione synthetase	0.00	1.0E+00
PRDX5	peroxiredoxin-5	1.95	1.8E-02
PRDX6	peroxiredoxin-6	3.27	3.8E-45

Table 2 Comparative transcriptomic analysis for the related genes of photosynthesis antenna protein of *Scenedesmus* under 70% and 1% CO_2 conditions.

Gene name	Enzyme	Log_2FC(70%/1%)	FDR
LHCA1	light-harvesting complex I	-4.18	1.2E-04
	chlorophyll a/b binding	-4.20	1.2E-04
	protein 1	-5.07	1.1E-06
LHCA2	light-harvesting complex I	-5.21	4.4E-07
	chlorophyll a/b binding	-4.56	2.1E-05
	protein 2		
LHCA3	light-harvesting complex I	-4.16	1.3E-04
	chlorophyll a/b binding	-4.33	5.6E-05
	protein 3		
LHCA4	light-harvesting complex I	-5.25	4.0E-08
	chlorophyll a/b binding	-4.80	4.6E-06
	protein 4	-5.06	8.9E-07
		-4.00	2.9E-04
LHCA5	light-harvesting complex I	-5.64	1.6E-08
	chlorophyll a/b binding	-4.59	1.5E-05
	protein 5	-4.74	8.0E-06
LHCB1	light-harvesting complex II	1.08	2.1E-19
	chlorophyll a/b binding	1.25	8.2E-32
	protein 1	2.37	4.4E-04
		2.00	1.0E-02

		-1.68	3.7E-02
LHCB2	light-harvesting complex II chlorophyll a/b binding protein 2	1.49	1.3E-31
LHCB4	light-harvesting complex II chlorophyll a/b binding protein 4	-4.36	5.6E-05
		-5.12	8.2E-07
LHCB5	light-harvesting complex II chlorophyll a/b binding protein 5	-4.15	1.5E-04

Table 3 Comparative transcriptomic analysis for the related genes of CO_2 fixation of *Scenedesmus* under 70% and 1% CO_2 conditions.

Gene name	Enzyme	Log2FC	FDR
GAPA	glyceraldehyde-3-phosphate dehydrogenase	-4.64	1.37E-05
		-4.11	1.76E-04
E2.2.1.1, tktA, tktB	transketolase	-5.60	1.55E-09
		-4.95	2.10E-06
FBP, fbp	fructose-1,6-bisphosphatase	-4.60	1.38E-05
PRK, prkB	phosphoribulokinase	-3.85	4.11E-04
		-3.72	9.02E-04
E3.1.3.37	Sedoheptulose-1,7-bisphosphatase	1.66	8.62E-07
		1.37	8.35E-05
		-5.95	4.72E-11
		-3.55	1.65E-03
rpe, RPE	ribulose-phosphate 3-epimerase	-4.69	9.04E-06
rbcL	ribulose-bisphosphate carboxylase large chain	1.38	2.41E-03
ALDO	fructose-bisphosphate aldolase, class I	-5.73	1.09E-08
GAPDH, gapA	Glyceraldehyde 3-phosphate dehydrogenase	-4.79	1.26E-06
		-1.65	6.68E-04
		-2.81	1.77E-02
		1.02	5.60E-06
MDH1	malate dehydrogenase, cytoplasmic	2.17	6.17E-72
		2.15	5.36E-07
MDH2	Malate dehydrogenase, glyoxysomal;	1.53	8.16E-26
		-5.20	5.68E-08
ppdK	pyruvate, orthophosphate dikinase	-4.93	3.85E-07
		1.17	5.38E-20
E1.1.1.40, maeB	NADP-dependent malic enzyme	1.05	6.78E-24
		2.96	3.30E-45
PGK, pgk	Phosphoglycerate kinase	-5.22	3.99E-07

		-4.86	2.80E-06
		-1.16	3.21E-02
		1.56	4.50E-24
		1.88	1.63E-55
E4.1.1.49, pckA	phosphoenolpyruvate carboxykinase	3.28	1.75E-45
		3.28	2.21E-43
		3.09	5.21E-30
		4.28	1.86E-29
		1.63	5.43E-24
		2.60	1.46E-05
		2.87	2.52E-23
		-5.76	4.06E-09
		-5.17	4.06E-07
E1.1.1.82	Malate dehydrogenase	-1.41	7.67E-14
		-1.55	1.70E-13
GOT1	aspartate aminotransferase, cytoplasmic	3.43	3.33E-78
		1.78	1.18E-32
		1.61	1.99E-22
GPT, ALT	alanine transaminase	1.33	7.41E-32
GGAT	glutamate--glyoxylate aminotransferase	1.11	5.38E-19
CAN	carbonic anhydrase 8	1.45	1.31E-14
	carbonic anhydrase 2	2.16	7.36E-36
	carbonic anhydrase 2	2.80	2.80E-07
	carbonic anhydrase 2	1.40	3.48E-03
	carbonic anhydrase 6	-2.84	1.51E-04
	Gamma carbonic anhydrase-like 1	-4.34	2.27E-05
	Gamma carbonic anhydrase 2	-5.04	2.47E-07
	Gamma carbonic anhydrase 3	-4.05	1.17E-04